Fluid Phase Behavior under supercritical conditions of Binary Systems in presence of Imidazolium and Ammonium Ionic Liquids

Edson M. S. Igarashi, Pedro F. Arce
Chemical Engineering Department, Engineering School of Lorena, University of Sao Paulo.

ABSTRACT
Ionic liquids have emerged recently as a friendly alternative for the environment by replacing volatile organic compounds in many separation processes. The main application of the ionic liquids is as solvents in processes, so the phase equilibria with other substances becomes an important piece of information to fully understand the behavior during an operation. Once that the carbon dioxide in supercritical conditions is frequently studied in separation processes, the thermodynamic modeling of binary systems formed by this substance with ionic liquids based on imidazolium or ammonium ions was proposed using cubic and non-cubic equations. Only the experimental data considered thermodynamic consistent according to the area test based on Gibbs-Duhem equation were modeled. The best results were obtained by the PC-SAFT thermodynamic model. The thermodynamic simulation using artificial neural networks nd molecular descriptors, using several architectures, was done. Results from the two approaches, ANN-MD and PC-SAFT models, were compared and the deviations in the bubble pressure and the vapor phase compositions were very similar being the computation time the main difference.

Keywords: imidazolium, ammonium, supercritical CO_2, thermodynamic modeling, thermodynamic simulation.

1 INTRODUCTION

The demand for supplies constantly rises as the population increases and the processes to obtain those products become harmful to the environment due to the quantities of solvents required. So, the retention of these compounds during the operation and the properly discard initiate an important environmental subject [1]. In this context, the ionic liquids (ILs) arises as a promising substitute because of their advantageous properties, among various applications, as solvents [2]. The ILs are considered a subset of molten salts with a melting point near to 100ºC and composed basically by a low symmetry organic cation and an organic or inorganic anion. So, an infinity of combinations is possible and the studies about these compounds and its applications have increased recently due to the specific properties that can be reached depending on the chosen structure of the ions [3-7].
In this work, the study of the fluid phase behavior was proposed for several binary systems containing supercritical CO_2 and ILs based on ammonium or imidazolium. Experimental data for these binary systems were obtained from the literature. First, the data were submitted to the thermodynamic consistency test. Second, only the data considered thermodynamically consistent were modeled using the equations of state of Peng-Robinson (PR) and the Perturbed Chain – Statistical Associating Fluid Theory (PC-SAFT) with properly mixture rules. The thermodynamic simulation, through the artificial neural networks (ANN) and molecular descriptors (MD), were also made. Results, in terms of the bubble pressure and vapor mole fraction deviations, are the lowest ones and very similar between the PC-SAFT EoS and the combination ANN-MD set.

2 METHODOLOGY

2.1 Thermodynamic models

2.2.1. Peng-Robinson EoS

The PR EoS [8] were combined with the classical van der Waals (vdW2) mixing rule that defines the energy and covolume constants of PR EoS, *a* and *b*:

$$a = \sum_i \sum_j x_i x_j a_{ij} \;\; ; \;\; a_{ij} = \sqrt{a_i a_j}\left(1 - k_{ij}\right) \; ; \; b = \sum_i \sum_j x_i x_j b_{ij} \; ; \; b_{ij} = \frac{1}{2}\left(b_i + b_j\right)\left(1 - l_{ij}\right) \qquad (1)$$

where the crossed parameters, a_{ij} and b_{ij}, depend on pure components parameters and binary interaction parameters, k_{ij} and l_{ij}. Pure component parameters (a_i and b_i) are calculated as presented in original work [8].

2.2.2. Perturbed Chain Statistical Associating Fluid Theory (PC-SAFT EoS)

The PC-SAFT EoS [9,10] calculates the residual Helmholtz free energy, $\tilde{a}^{res}$, from the summation of three terms: a reference hard-sphere chain ($\tilde{a}^{hc}$), a perturbation contribution, $\tilde{a}^{pert}$, and associating contribution, $\tilde{a}^{assoc}$, where $\tilde{a} = A / NkT$. Conventional combining rules are used to determine the cross parameters:

$$\sigma_{ij} = \frac{1}{2}\left(\sigma_{ii} + \sigma_{jj}\right) \;\; ; \;\; \varepsilon_{ij} = \sqrt{\varepsilon_{ii}\varepsilon_{jj}}\left(1 - k_{ij}\right) \qquad (2)$$

where k_{ij} is the adjustable parameter which evaluates the interaction between molecules. The whole thermodynamic model can be seen in the literature [9,10].

2.2 Thermodynamic consistency

A thermodynamic consistency test based on Gibbs-Duhem equation (Eq. 3) were used, in order to increase the reliability of the data to be modeled [11,12]. The equation of state of Peng-Robinson associated to van der Walls mixing rule with one binary interaction parameter was combined to calculate the necessary variables. In this case, the integral test was used for being suitable for isothermal systems with very small fractions of the solute in the vapor phase under higher pressures [11].

$$\int \frac{1}{P y_2} dP = \int \frac{(1-y_2)}{y_2(Z-1)} \frac{d\hat{\phi}_1}{\hat{\phi}_1} + \int \frac{1}{(Z-1)} \frac{d\hat{\phi}_2}{\hat{\phi}_2} \qquad (3)$$

Where each side of the equation 1 generates a term of the area that is correlated to calculate the area for each experimental data set, as shown in Eq. 4.

$$A_P = \int \frac{1}{P y_2} dP \;, \qquad A_\phi = \int \frac{(1-y_2)}{y_2(Z-1)} \frac{d\hat{\phi}_1}{\hat{\phi}_1} + \int \frac{1}{(Z-1)} \frac{d\hat{\phi}_2}{\hat{\phi}_2}, \qquad \%\Delta A = 100.\left(\frac{A_\phi - A_P}{A_P}\right) \qquad (4)$$

The criterium adopted was that the experimental data set with $\%\Delta A$ between -20% and 20% was considered thermodynamic consistent. Only the data considered thermodynamic consistent proceeded to the thermodynamic modeling.

2.3 Thermodynamic modeling

The most common method for the prediction of phase equilibria in systems with supercritical fluids is the application of an EoS.

From the isofugacity condition in the ϕ-ϕ approach, the starting point for VLE calculation is:

$$x_i \hat{\phi}_i^L(T, P, x_i) = y_i \hat{\phi}_i^V(T, P, y_i) \qquad (5)$$

Here the superscripts L and V represent liquid and vapor, respectively, y_i and x_i are the mole fraction of species *i* in the vapor and in the liquid phases and $\hat{\phi}_i$ is the fugacity coefficient of species *i*. A cubic EoS can be used to obtain the fugacity coefficient in the vapor and liquid phases in terms of temperature, pressure, and concentration.

2.4 Thermodynamic simulation

The thermodynamic simulation was done by using the ANN [13] with different architectures combined with molecular descriptors (MD) [14] in order to improve the chemical descriptions of the binary systems. Thermodynamic properties of ILs are analyzed to study the capabilities of artificial neural networks (ANNs) to learn, test and predict the fluid phase behavior properties: bubble pressure and the vapor phase composition. For the ANN method developed in this research, the main learning variables are the critical properties of ILs (Pc, Tc, and w), temperature and liquid phase composition of the systems. All of these properties are considered as independent variables to define the fluid phase behavior of these binary

systems: IL + supercritical CO_2. To distinguish between the chemical characteristics of the ILs studied in this work, molecular descriptors were obtained from the computational chemistry (Dragon 7) and were also considered as independent variables. In this work, two types of the cation of ILs with several anions were studied. First, in accord to the molecular structure of the IL, it was found the SMILES code of each IL. Second, with the SMILE code known, there were obtained, using the Dragon 7, the numeric value for the selected molecular descriptors.

For learning, testing and predicting the fluid phase behavior properties of two cation types of ILs, a spreadsheet file (MS-Excel) with six worksheets, each one with special function, was used. The first, third and fifth worksheets for the learning, testing and predictions steps, respectively, contain the independent variables. The second, fourth and sixth worksheets for the learning, testing and prediction steps, respectively, contain the dependent variables. Data and number of data are different for the first, third and fifth worksheets. A computer program for three dependent variables, in MatLab, was developed by one of the authors that interact with each worksheet of the spreadsheet file. In this form, to obtain the best architecture, several network architectures were studied.

3 RESULTS

The binary systems were composed by supercritical CO_2 and ILs. The ILs studied are shown in Table 1. The critical properties were obtained from the original work. In the cases that the information was not provided, it was calculated through the methods proposed by Valderrama and co-workers [15, 16], as shown in Table 2. The physical descriptions of the systems investigated in this study are shown in Table 3, where NP means the number of experimental points.

Table 1. imidazolium and ammonium ILs used in this work

Ionic liquids	Abbreviation
1-butyl-3-methylimidazolium dicyanamide	[C4mim][DCA]
1-butyl-3-methylimidazolium bis(trifluoromethylsulfonyl)imide	[C4mim][Tf2N]
1-ethyl-3-methylimidazolium hexafluorophosphate	[emim][PF_6]
1-hexyl-3-methylimidazolium hexafluorophosphate	[hmim][PF6]
1-octyl-3-methylimidazolium tetrafluoroborate	[omim][BF_4]
N,n-diethyl-n-methyl-n-propylammonium bis(fluorosulfonyl)imide	[N1223][FSI]
N-methyl-2-hydroxyethylammonium acetate	m-2-HEAA
N-methyl-2-hydroxyethylammonium formate	m-2-HEAF
2-hydroxy ethylammonium acetate	HEA
2-hydroxy ethylammonium lactate	HEL
Bis(2-hydroxyethyl)ammonium acetate	BHEAA
Bis(2-hydroxyethyl)ammonium lactate	BHEAL
2-Hydroxy-N-(2-hydroxyethyl)-N-methylethanaminium acetate	HHEMEA
2-Hydroxy-N-(2-hydroxyethyl)-N-methylethanaminium lactate	HHEMEL
2-hydroxy ethylammonium formate	HEF
2-(2-hydroxy ethoxy) ammonium formate	HEAF
2-(2-hydroxy ethoxy) ammonium acetate	HEAA
2-(2-hydroxy ethoxy) ammonium lactate	HEAL
Tri-(2-hidroxy ethyl) ammonium acetate	THEAA
Tri-(2-hidroxy ethyl) ammonium lactate	THEAL

Table 2. Critical properties and acentric factor of the ILs for the binary systems

Component	PR EoS			PC-SAFT EoS [b]				
	Tc [K]	Pc [MPa]	w	m/MW [mol^{-1}]	σ [10^{+10} m]	ε/k [K]	$k^{A\,B}$	$\varepsilon^{A\,B}/k$ [K]
CO_2 [25]	304.21	7.38	0.2236	2.0514	2.8145	168.74	---	---
[C4mim][DCA] [17]	782.96	2.44	0.8419	3.8052	3.8052	282.63	1885.75	0.0291
[C4mim][Tf2N] [17]	826.30	2.76	0.3004	3.4030	3.3128	265.74	1956.81	0.0415
[emim][PF6] [15]	663.50	1.95	0.6708	3.9007	4.0921	268.81	2029.74	0.0218
[hmim][PF6] [15]	754.30	1.55	0.8352	3.8457	3.4051	354.38	2053.68	0.0512
[omim][BF4] [15]	726.10	1.60	0.9954	4.1541	3.1345	327.18	2156.79	0.0408
[N1223][FSI] [21]	1059.8	4.22	0.3563	4.5270	3.8712	352.75	2212.84	0.0316
m-2-HEAA [22]	715.66	3.33	0.9836	4.7107	4.2130	315.60	2215.60	0.0364
m-2-HEAF [22]	698.95	4.14	0.9359	5.1352	4.0135	328.54	2083.58	0.0515
HEA [a]	699.20	4.14	0.9359	5.7458	3.8720	339.48	2063.45	0.0454
HEL [a]	812.60	3.94	1.3579	5.2152	3.9711	312.67	2138.70	0.0592

BHEAA [a]	829.30	3.18	1.4044	6.1385	4.1341	329.79	2215.11	0.0434
BHEAL [a]	946.90	3.06	1.7485	5.3120	3.7954	348.74	2186.93	0.0522
HHEMEA [a]	828.70	3.00	1.3799	5.7745	3.4358	322.78	2089.48	0.0615
HHEMEL [a]	946.70	2.89	1.7149	6.4974	4.4910	340.45	2122.53	0.0545
HEF [a]	571.30	4.96	0.8477	5.9412	3.8922	372.84	2092.43	0.0563
HEAF [a]	645.60	3.66	0.9187	5.6182	4.1608	342.74	1989.72	0.0574
HEAA [a]	770.10	3.20	1.0138	7.8523	4.4501	334.85	2136.25	0.0489
HEAL [a]	883.10	3.07	1.4074	7.3412	3.8713	343.70	2268.39	0.0436
THEAA [a]	946.10	2.85	1.7229	8.6162	3.7616	344.63	2165.33	0.0540
THEAL [a]	1071.7	2.74	1.9075	8.3108	4.3015	373.96	1996.75	0.0632

[a] Calculated in this work using the method proposed by Valderrama and coworkers [15,16]

[b] All PC-SAFT pure component parameters were calculated in this work

Table 3. Physical characteristics of the binary systems studied in this work

System	NP	ΔT [K]	ΔP [MPa]	Δx_1	Ref.
CO_2 + imidazolium ILs					
CO_2 + ⌈C4mim⌉⌈DCA⌉	40	293.4 – 363.2	1.02 – 73.64	0.2000 – 0.6010	[17]
CO_2 + [C4mim][Tf2N]	68	292.6 – 363.3	0.63 – 49.99	0.2310 – 0.8010	[17]
CO_2 + [emim][PF6]	70	313.0 – 352.9	1.49 – 97.10	0.1040 – 0.619	[18]
CO_2 + [hmim][PF6]	97	298.3 – 363.6	0.64 – 94.60	0.0980 – 0.7270	[19]
CO_2 + ⌈omim⌉[BF4]	91	308.2 – 363.3	0.57 – 85.80	0.1005 – 0.7523	[20]
CO_2 + ammonium ILs					
CO_2 + ⌈N1223⌉⌈FSI⌉	36	298.2 – 343.2	0.01 – 1.90	0.0020 – 0.3540	[21]
CO_2 + m-2-HEAA	42	312.3 – 363.6	0.84 – 80.50	0.1570 – 0.5000	[22]
CO_2 + m-2-HEAF	80	293.2 – 363.4	0.49 – 52.91	0.0570 – 0.5340	[22]
CO_2 + HEA	18	298.2 – 328.2	0.12 – 1.54	0.0081 – 0.1442	[23]
CO_2 + BHEAA	18	298.2 – 328.2	0.13 – 1.52	0.0074 – 0.1076	[23]
CO_2 + HHEMEA	18	298.2 – 328.2	0.12 – 1.54	0.0024 – 0.0761	[23]
CO_2 + HEL	18	298.2 – 328.2	0.13 – 1.56	0.0034 – 0.1056	[23]
CO_2 + BHEAL	18	298.2 – 328.2	0.12 – 1.60	0.0035 – 0.0835	[23]
CO_2 + HHEMEL	18	298.2 – 328.2	0.15 – 1.56	0.0027 – 0.0776	[23]
CO_2 + HEF	27	303.0 – 323.0	0.44 – 10.01	0.0271 – 0.3083	[24]
CO_2 + HEA	24	303.0 – 323.0	0.89 – 10.98	0.0316 – 0.4009	[24]
CO_2 + HEL	24	303.0 – 323.0	0.78 – 10.09	0.0260 – 0.2422	[24]
CO_2 + THEAA	24	303.0 – 323.0	1.03 – 10.12	0.0345 – 0.2561	[24]
CO_2 + THEAL	21	303.0 – 323.0	0.96 – 8.47	0.0835 – 0.4617	[24]
CO_2 + HEAF	21	303.0 – 323.0	0.66 – 8.52	0.0202 – 0.1907	[24]
CO_2 + HEAA	24	303.0 – 323.0	0.76 – 7.67	0.0680 – 0.4860	[24]
CO_2 + HEAL	21	303.0 – 323.0	1.24 – 8.50	0.0559 – 0.2640	[24]

3.1 Thermodynamic modeling and simulation.

In Table 4, the SMILES codes for the imidazolium and ammonium ILs used for studying the fluid phase behavior of binary systems at high-pressures, are shown. In Table 5, the selected molecular descriptors are briefly described. This table shows the blocks and sub-blocks to which the molecular descriptor belongs. Numerical values for the molecular descriptors of the imidazolium and ammonium ILS, calculated by the Dragon using the SMILES codes, are shown in Table 6.

Table 4. SMILES codes for the imidazolium and ammonium ILs used in this work

Ionic liquids	SMILES code
⌈C4mim⌉⌈DCA⌉	CCCC[n+]1CCn(C)C1.N#C[N-]C#N
[C4mim][Tf2N]	CCCCn1CC[n+](C)C1.FC(F)(F)[S](=O)(=O)[N-][S](=O)(=O)C(F)(F)F
[emim][PF_6]	CC[n+]1CCn(C)C1.F[P-](F)(F)(F)(F)F
[hmim][PF6]	CCCCCC[n+]1CCn(C)C1.F[P-](F)(F)(F)(F)F
[omim][BF_4]	CCCCCCCC[n+]1CCn(C)c1.F[B-](F)(F)F
[N1223][FSI]	CCC[N+](C)(CC)CC.F[S](=O)(=O)[N-][S](F)(=O)=O
m-2-HEAA	C[NH2+]CCO.CC([O-])=O
m-2-HEAF	CC(O)C([O-])=O.OCC[NH+](CCO)CCO
HEA	CC([O-])=O.[NH3+]CCO
HEL	CC(O)C([O-])=O.[NH3+]CCO
BHEAA	CC([O-])=O.OCC[NH2+]CCO
BHEAL	CC(O)C([O-])=O.OCC[NH2+]CCO
HHEMEA	C[NH+](CCO)CCO.CC([O-])=O
HHEMEL	CC(O)C([O-])=O.C[NH+](CCO)CCO
HEF	[NH3+]CCO.[O-]C=O

HEAF	[NH3+]CCOCCO.[O-]C=O
HEAA	CC([O-])=O.[NH3+]CCOCCO
HEAL	CC(O)C([O-])=O.[NH3+]CCOCCO
THEAA	CC([O-])=O.OCC[NH+](CCO)CCO
THEAL	CC(O)C([O-])=O.OCC[NH+](CCO)CCO

Table 5. Description of molecular descriptors selected in this work.

Name	Description	Block	Sub-Block
AMW	average molecular weight	Constitutional indices	Basic descriptors
nH	number of Hydrogen atoms		
nC	number of Carbon atoms		
nN	number of Nitrogen atoms		
nF	number of Fluorine atoms		
Pol	polarity number		
XMOD	solvation connectivity index of order 1	Connectivity indices	Solvation connectivity indices
RDCHI	modified Randic index		Randic-like connectivity indices
P_VSA	reciprocal distance sum Randic-like index		

Table 6. Values for the molecular descriptors of imidazolium and ammonium ILs used in this work

Ionic liquids	AMW	nH	nC	nN	nF	Pol	XMOD	RDCHI	P_VSA
[C4mim][DC	6.313	18	10	5	0	10	45.956	3.741	211.88
[C4mim][Tf2	9.824	18	10	3	6	32	90.395	4.419	211.88
[emim][PF_6]	8.938	14	6	2	6	6	53.657	3.241	164.795
[hmim][PF6]	7.690	22	10	2	6	10	65.657	3.835	258.964
[omim][BF_4]	6.459	25	12	2	4	12	56.263	4.075	294.278
[N1223][FSI	8.169	20	8	2	2	16	70.504	3.585	235.422
m-2-HEAA	6.145	13	5	1	0	2	27.343	2.734	117.711
m-2-HEAF	6.468	21	9	1	0	13	49.399	3.605	188.338
HEA	6.377	11	4	1	0	1	24.093	2.559	82.398
HEL	6.573	13	5	1	0	5	30.134	2.809	94.169
BHEAA	6.355	15	6	1	0	4	33.947	3.065	129.482
BHEAL	6.508	17	7	1	0	8	39.988	3.315	141.253
HHEMEA	6.181	17	7	1	0	6	36.507	3.103	164.795
HHEMEL	6.342	19	8	1	0	10	42.548	3.353	176.567
HEF	6.696	9	3	1	0	1	22.445	2.489	58.856
HEAF	6.573	13	5	1	0	4	32.445	2.995	105.94
HEAA	6.355	15	6	1	0	4	34.093	3.065	129.482
HEAL	6.508	17	7	1	0	8	40.134	3.315	141.253
THEAA	6.342	19	8	1	0	9	43.357	3.355	176.567
THEAL	6.468	21	9	1	0	13	49.399	3.605	188.338

Results of the thermodynamic consistency tests are shown in Table 7 with the results of the thermodynamic modeling and simulation of the fluid phase behavior of the vapor-liquid equilibrium. NPTC is the number of experimental points considered thermodynamic consistent. The average deviations are expressed as $\%\Delta P$ and $\%\Delta y_1$ for the bubble pressure and vapor phase composition, respectively, using the PR and the PF-SAFT models. In this table, the results of the thermodynamic simulation are shown for the best configuration of four layers (10-15-10-2). In this configuration, 10 represents the number of independent variables (temperature, liquid phase composition, critical properties, and molecular descriptors), 15 and 10 represent the hidden layers, and 2 represents the number of dependent variables (bubble pressure and the vapor phase composition).

Table 7. Results obtained for the thermodynamic modeling and simulation of several binary systems involving imidazolium and ammonium ILs and supercritical CO_2

System: CO_2 +	NP	NPTC	T [K]	PR EoS				PC-SAFT EoS			ANN	
				k_{ij}	l_{ij}	ΔP^a	$\Delta y_1{}^b$	k_{ij}	ΔP^a	$\Delta y_1{}^b$	ΔP^a	$\Delta y_1{}^b$
[C4mim][DCA]	5	4	293.4	0.1186	0.0420	2.55	0.00	0.0812	0.58	0.00	0.50	0.00
	5	4	303.3	0.1240	0.0380	2.47	0.00	0.0705	0.47	0.00	0.41	0.00
	5	4	313.2	0.1413	0.0401	1.89	0.00	0.0712	0.68	0.00	0.62	0.00
	5	4	323.1	0.1685	0.0426	7.94	0.00	0.0698	0.51	0.00	0.41	0.00
	5	4	333.1	0.1615	0.0327	8.34	0.00	0.0705	0.63	0.00	0.52	0.00
	5	4	343.2	0.2024	0.0475	10.12	0.00	0.0683	0.94	0.00	0.64	0.00

	5	4	353.1	0.0858	-0.0160	19.72	0.00	0.0678	0.79	0.00	0.51	0.00
	5	4	363.2	0.1736	0.0348	3.82	0.00	0.0689	0.80	0.00	0.53	0.00
[C4mim] [Tf_2N]	9	8	293.3	0.0760	0.0899	17.40	0.00	0.0325	0.68	0.00	0.60	0.00
	9	9	303.2	0.1268	0.1179	25.93	0.00	0.0421	0.74	0.00	0.63	0.00
	9	9	313.2	0.1668	0.1471	36.19	0.00	0.0398	0.86	0.00	0.59	0.00
	9	8	323.2	0.0638	0.0653	22.42	0.00	0.0354	0.81	0.00	0.61	0.00
	8	8	333.2	-0.0031	0.0101	28.24	0.03	0.0382	0.80	0.00	0.58	0.00
	8	8	343.1	0.0488	0.0489	22.13	0.05	0.0371	0.68	0.00	0.59	0.00
	8	8	353.2	0.0420	0.0452	23.16	0.10	0.0380	0.61	0.00	0.52	0.00
	8	8	363.2	0.1715	0.1360	12.83	0.20	0.0392	0.75	0.00	0.57	0.00
[emim] [PF_6]	6	3	313.1	0.3177	0.1320	31.54	0.01	0.0312	0.71	0.00	0.63	0.00
	6	3	318.0	0.2704	0.0826	34.71	0.02	0.0307	1.03	0.00	0.80	0.00
	8	5	323.0	0.2757	0.0652	20.67	0.03	0.0311	0.88	0.00	0.57	0.00
	8	5	328.0	0.2647	0.0458	23.34	0.05	0.0323	0.95	0.00	0.66	0.00
	9	6	332.9	0.2489	0.0347	23.10	0.04	0.0303	1.04	0.00	0.83	0.00
	8	7	342.9	0.1653	-0.0366	44.71	0.11	0.0292	0.81	0.00	0.65	0.00
	8	7	347.8	0.1520	-0.0422	43.89	0.12	0.0287	0.87	0.00	0.62	0.00
	8	6	352.7	0.1501	-0.0469	40.59	0.14	0.0308	0.90	0.00	0.58	0.00
[hmim] [PF_6]	2	2	298.4	0.1234	0.0257	0.03	0.00	0.0584	0.65	0.00	0.47	0.00
	3	3	304.4	0.1269	0.0260	0.60	0.00	0.0560	0.52	0.00	0.41	0.00
	4	4	308.4	0.1261	0.0228	1.91	0.00	0.0563	0.82	0.00	0.60	0.00
	9	6	313.2	0.1638	0.0326	13.04	0.00	0.0574	0.69	0.00	0.52	0.00
	10	7	318.2	0.1583	0.0344	11.78	0.00	0.0561	1.06	0.00	0.75	0.00
	10	7	323.2	0.1919	0.0434	13.55	0.00	0.0558	0.89	0.00	0.61	0.00
	10	7	328.2	0.1803	0.0370	14.43	0.00	0.0560	1.08	0.00	0.67	0.00
	10	7	333.1	0.1470	0.0228	16.20	0.00	0.0562	0.74	0.00	0.59	0.00
	10	7	338.1	0.1644	0.0221	16.12	0.00	0.0557	0.83	0.00	0.55	0.00
	9	6	343.1	0.1494	0.0104	12.41	0.00	0.0552	0.92	0.00	0.62	0.00
	7	6	348.2	0.2046	0.0378	8.42	0.01	0.0554	1.06	0.00	0.63	0.00
	5	5	353.3	0.1297	0.0116	4.64	0.00	0.0559	0.72	0.00	0.48	0.00
	4	4	358.6	0.1801	0.0275	0.93	0.00	0.0551	0.76	0.00	0.52	0.00
	4	4	363.4	0.1877	0.0280	1.41	0.00	0.0550	0.80	0.00	0.61	0.00
[omim] [BF_4]	5	5	308.4	0.1098	0.0281	1.00	0.00	0.0365	0.35	0.00	0.18	0.00
	8	7	313.2	0.1452	0.0407	11.50	0.00	0.0369	0.68	0.00	0.37	0.00
	8	7	318.5	0.0547	-0.0008	24.50	0.00	0.0371	0.74	0.00	0.41	0.00
	7	7	323.2	0.1342	0.0340	14.05	0.00	0.0367	0.63	0.00	0.43	0.00
	8	7	328.0	0.1378	0.0316	15.19	0.01	0.0363	0.49	0.00	0.27	0.00
	8	7	333.4	0.1191	0.0218	18.02	0.01	0.0369	0.89	0.00	0.53	0.00
	7	7	338.0	0.1196	0.0197	17.59	0.00	0.0371	1.03	0.00	0.78	0.00
	9	8	343.0	0.0394	-0.0112	22.11	0.01	0.0373	1.07	0.00	0.81	0.00
	8	6	348.3	0.1561	0.0363	2.68	0.02	0.0369	0.62	0.00	0.42	0.00
	7	6	353.0	0.1606	0.0364	2.47	0.02	0.0374	0.38	0.00	0.21	0.00
	8	6	358.0	0.1655	0.0367	2.43	0.03	0.0369	0.41	0.00	0.19	0.00
	8	6	362.9	0.1707	0.0373	2.40	0.03	0.0366	0.33	0.00	0.17	0.00
[N1223] [FSI]	12	12	298.2	-0.0208	0.0148	2.22	0.00	0.1021	0.87	0.00	0.54	0.00
	12	12	313.2	-0.0213	0.0153	0.79	0.00	0.1136	0.61	0.00	0.36	0.00
	12	12	343.2	0.0665	0.0472	11.41	0.00	0.1085	0.89	0.00	0.47	0.00
m-2-HEAA	7	6	313.2	0.1939	0.0877	15.54	0.00	0.0854	1.02	0.00	0.74	0.00
	7	6	323.3	0.2041	0.0881	14.87	0.00	0.0923	0.98	0.00	0.64	0.00
	7	6	333.4	0.2037	0.0825	13.27	0.00	0.0954	0.85	0.00	0.53	0.00
	7	6	343.3	0.1508	0.0531	16.95	0.00	0.1032	1.03	0.00	0.81	0.00
	7	6	353.3	0.0501	0.0011	30.63	0.00	0.1008	1.05	0.00	0.75	0.00
	7	6	363.3	0.1841	0.0626	2.89	0.01	0.1158	0.32	0.00	0.18	0.00
m-2-HEAF	10	9	293.3	0.0295	-0.0154	18.80	0.00	0.0785	0.85	0.00	0.49	0.00
	10	10	303.2	0.0410	-0.0131	21.37	0.00	0.0841	1.01	0.00	0.80	0.00
	10	10	313.3	0.0486	-0.0157	20.23	0.00	0.0823	0.81	0.00	0.61	0.00
	10	10	323.2	0.0629	-0.0108	17.37	0.00	0.0895	1.03	0.00	0.79	0.00
	10	10	333.3	0.0586	-0.0136	17.54	0.00	0.0901	0.75	0.00	0.51	0.00
	10	10	343.3	-0.1062	-0.0751	39.38	0.00	0.0887	0.84	0.00	0.49	0.00
	10	10	353.3	0.0265	-0.0313	20.76	0.01	0.0906	1.02	0.00	0.83	0.00
	10	10	363.3	0.0177	-0.0450	22.80	0.01	0.0912	0.87	0.00	0.62	0.00
HEA[c]	6	6	298.2	0.0213	-0.0022	0.56	0.00	0.1236	0.23	0.00	0.16	0.00
	6	6	313.2	0.0001	-0.0037	0.76	0.00	0.1141	0.18	0.00	0.12	0.00
	6	6	328.2	-0.0420	-0.0238	1.67	0.00	0.1159	0.60	0.00	0.34	0.00
HEL[c]	6	6	298.2	-0.0129	-0.0070	0.60	0.00	0.1021	0.32	0.00	0.18	0.00
	6	6	313.2	-0.0006	-0.0011	0.91	0.00	0.0975	0.27	0.00	0.13	0.00
	6	6	328.2	0.0059	-0.0212	1.35	0.00	0.1008	0.31	0.00	0.19	0.00

	6	6	298.2	0.0033	-0.0124	0.68	0.00	0.1232	0.33	0.00	0.18	0.00
BHEAA	6	6	313.2	-0.0096	-0.0138	0.75	0.00	0.1285	0.24	0.00	0.13	0.00
	6	6	328.2	0.0041	-0.0162	0.50	0.00	0.1321	0.18	0.00	0.11	0.00
	6	6	298.2	0.0010	-0.0075	0.50	0.00	0.1033	0.26	0.00	0.14	0.00
BHEAL	6	6	313.2	-0.0466	-0.0165	0.41	0.00	0.1121	0.19	0.00	0.12	0.00
	6	6	328.2	0.1487	0.0068	0.83	0.00	0.1274	0.33	0.00	0.21	0.00
	6	6	298.2	0.0535	-0.0138	0.57	0.00	0.1320	0.17	0.00	0.12	0.00
HHEMEA	6	6	313.2	0.0421	-0.0184	0.66	0.00	0.1287	0.20	0.00	0.13	0.00
	6	6	328.2	-0.2585	-0.1150	2.57	0.00	0.1196	0.35	0.00	0.17	0.00
	6	6	298.2	0.0025	-0.0121	0.50	0.00	0.1025	0.17	0.00	0.13	0.00
HHEMEL	6	6	313.2	0.0026	-0.0133	0.56	0.00	0.1036	0.16	0.00	0.10	0.00
	6	6	328.2	-0.1004	-0.0481	0.75	0.00	0.0985	0.23	0.00	0.08	0.00
	9	9	303.0	0.2084	0.0720	1.81	0.04	0.0874	0.19	0.00	0.09	0.00
HEF	9	9	313.0	0.2907	0.1127	3.99	0.09	0.0895	0.26	0.00	0.10	0.00
	9	9	323.0	0.3158	0.1154	4.57	0.13	0.0812	0.31	0.00	0.13	0.00
	8	8	303.0	0.1052	0.0224	2.28	0.00	0.0623	0.32	0.00	0.20	0.00
HEA[d]	8	8	313.0	0.1572	0.0377	2.65	0.00	0.0740	0.30	0.00	0.21	0.00
	8	8	323.0	0.2008	0.0483	5.94	0.00	0.0785	0.27	0.00	0.17	0.00
	8	8	303.0	0.0567	0.0054	4.48	0.00	0.0871	0.36	0.00	0.18	0.00
HEL[d]	8	8	313.0	0.1449	0.0262	4.21	0.00	0.0886	0.21	0.00	0.11	0.00
	8	8	323.0	0.2023	0.0429	3.86	0.00	0.0907	0.25	0.00	0.14	0.00
	7	7	303.0	0.2754	0.0471	2.32	0.00	0.1032	0.41	0.00	0.19	0.00
HEAF	7	7	313.0	0.3213	0.0537	1.26	0.00	0.1007	0.32	0.00	0.21	0.00
	7	7	323.0	0.3074	0.0341	3.25	0.01	0.1012	0.28	0.00	0.17	0.00
	8	8	303.0	0.0647	0.0163	1.38	0.00	0.1362	0.30	0.00	0.22	0.00
HEAA	8	8	313.0	0.0763	0.0185	1.83	0.00	0.1208	0.28	0.00	0.16	0.00
	8	8	323.0	0.0810	0.0191	1.27	0.00	0.1038	0.18	0.00	0.07	0.00
	7	6	303.0	0.1022	0.0089	2.36	0.00	0.1320	0.41	0.00	0.20	0.00
HEAL	7	7	313.0	0.1434	0.0204	2.04	0.00	0.1424	0.38	0.00	0.19	0.00
	7	7	323.0	0.0984	0.0071	4.06	0.00	0.1386	0.48	0.00	0.21	0.00
	8	7	303.0	0.1453	0.0195	4.19	0.00	0.1241	0.47	0.00	0.18	0.00
THEAA	8	8	313.0	0.0992	0.0042	2.54	0.00	0.1432	0.29	0.00	0.16	0.00
	8	8	323.0	0.1001	0.0012	4.73	0.00	0.1387	0.41	0.00	0.18	0.00
	7	7	303.0	-0.0286	0.0029	1.70	0.00	0.0985	0.31	0.00	0.17	0.00
THEAL	7	7	313.0	-0.0341	0.0031	1.72	0.00	0.0856	0.25	0.00	0.12	0.00
	7	7	323.0	-0.0311	0.0035	1.47	0.00	0.1041	0.20	0.00	0.11	0.00

a: $\Delta P = \frac{100}{NPTC}\sum_1^{NPTC}\frac{|P^{exp}-P^{calc}|_i}{P_i^{exp}}$; b: $\Delta y_1 = \frac{100}{NPTC}\sum_1^{NPTC}\frac{|{y_1}^{exp}-{y_1}^{calc}|_i}{y_{1,i}^{exp}}$; c: [23]; d: [24]

In Figure 1, experimental data and results are presented for the thermodynamic modeling (PR and PC-SAFT EoS) and the predicted results obtained with the ANNs for two binary systems: (a) CO_2 + [C4mim][Tf_2N] at 363.2 K and (b) CO_2 + m-2-HEAA at 363.4 K. It is easy to appreciate the good agreement presented by the PC-SAFT Eos and the ANN model for modeling and predicting the vapor phase, while the results obtained with the PR EoS have a poor behavior in the vapor phase.

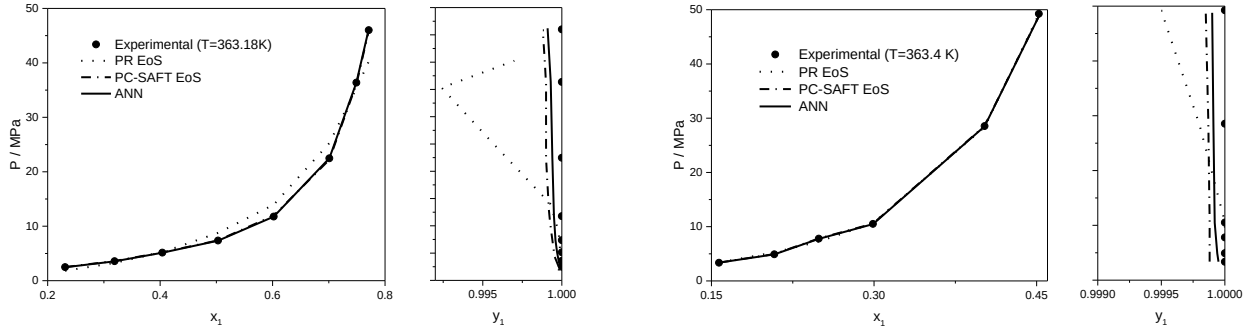

(a) **(b)**

Figure 1. Results for the fluid phase behavior of the system: (a) CO_2 + [C4mim][Tf_2N] at 363.2 K, (b) CO_2 + m-2-HEAA at 363.4 K

4 CONCLUSIONS

Experimental data, obtained from the literature, are submitted to the thermodynamic consistency to determine the experimental points considered consistent from the point of view of the thermodynamics, through of the Gibbs-Duhem equation. From the molecular configuration of imidazolium and ammonium ILs, the SMILES code could be obtained and from these, the values of the molecular descriptors were predicted by the Dragon. It is possible to model thermodynamically, using cubic and non-cubic EoS, the fluid phase behavior of systems containing imidazolium and ammonium ILs under supercritical conditions using CO_2 as a solvent. On the other hand, it is also possible to predict the bubble pressure and vapor phase composition using artificial neural networks and molecular descriptors through the optimum architecture. From the numerical results, it can be deduced that the PC-SAFT EoS and the ANN are the models that showed more success for the thermodynamic modeling and simulation of the fluid phase behavior in terms of the deviation in the bubble pressure and the vapor phase composition.

ACKNOWLEGMENTS

The financial supports of the Fundação de Amparo à Pesquisa do Estado de São Paulo, FAPESP (Brazil), through grants 2015/05155-8 and 2018/01511-2, are gratefully acknowledged.

REFERENCES

[1] VEKARIYA, R. L., A review of ionic liquids: applications towards catalytic organic transformations, J. Mol. Liq., Vol. 227, p. 44.
[2] LEI, Z. et al., Introduction: ionic liquids, Chem. Rev., Vol. 117, p. 6633.
[3] WANG, B. et al., Are ionic liquids chemically stable?, Chem. Rev., Vol. 117, p. 7113.
[4] BRANCO, L. C., Líquidos iónicos: aplicações e perspectivas futuras. In: ANO INTERNCIONAL DA LUZ 2015. Lisboa, Portugal: Química, Vol. 139, p. 15.
[5] ROGERS, R. D.; SEDDON, K. R., Ionic liquids – solvents of the future?, Science, Vol. 302, p. 792.
[6] DONG, K. et al. Multiscale studies on ionic liquids, Chem. Rev., Vol. 117, p. 6636.
[7] MARSH, K. N.; BOXALL, J. A.; LICHTENTHALER, R., Room temperature ionic liquids and their mixtures – a review, Fluid Phase Equilibr., Vol. 219, p. 93.
[8] PENG, D. Y.; ROBINSON, D. B., A new two-constant equation of state, Ind. Eng. Chem. Fundam., Vol. 15, p. 59.
[9] GROSS, J.; SADOWSKI, G., Application of perturbation theory to a hard-chain reference fluid: an equation of state for square-well chains, Fluid Phase Equilibr., Vol. 168, p. 183.
[10] GROSS, J.; SADOWSKI, G., Perturbed-chain SAFT: an equation of state based on a perturbation theory for chain molecules, Ind. Eng. Chem. Res., Vol. 40, p. 1244.
[11] ÀLVAREZ, V. H.; AZNAR, M., Application of a thermodynamic consistency test to binary mixtures containing an ionic liquid, The Open Thermodynamics Journal, Vol. 2, p. 25.
[12] VALDERRAMA, J. O.; FORERO, L. A.; ROJAS, R. E., Critical properties and normal boiling temperature of ionic liquids. Update and a new consistency test, Ind. Eng. Chem. Res., Vol. 51, p. 7838.
[13] da SILVA, I. N.; SPATTI, D. N.; FLAUZINO, R. A.; LIBONI, L. H.; ALVES, S. F., Artificial neural networks – A practical course; Springer International Publishing Switzerland, 2017
[14] DANISHUDDIN, A.; KHAN, A. U. Descriptors and their selection methods in QSAR analysis: paradigm for drug design, Drug Discov. Today, Vol. 21, p. 1291.
[15] VALDERRAMA, J. O.; ROBLES, P. A., Critical properties, normal boiling temperatures, and acentric factors of fifty ionic liquids, Ind. Eng. Chem. Res., Vol. 46, p. 1338.
[16] VALDERRAMA, J. O.; FORERO, L. A.; ROJAS, R. E., Extension of a group contribution method to estimate the critical properties of ionic liquids of high molecular mass, Ind. Eng. Chem. Res., Vol. 54, p. 3480.
[17] CARVALHO, P. J. et al., High pressure phase behavior of carbon dioxide in 1-butyl-3-methylimidazolium bis(trifluoromethylsulfonyl)imide and 1-butyl-3-methylimidazolium dicyanamide ionic liquids, J. Supercrit. Fluid., Vol. 50, p. 105.
[18] SHARIATI, A.; PETERS, C. J., High-pressure phase behavior of systems with ionic liquids: II. The binary system carbon dioxide+1-ethyl-3-methylimidazolium hexafluorophosphate, J. Supercrit. Fluid., Vol. 29, p. 43.
[19] SHARIATI, A.; PETERS, C. J., High-pressure phase behavior of systems with ionic liquids Part III. The binary system carbon dioxide + 1-hexyl-3-methylimidazolium hexafluorophosphate, J. Supercrit. Fluid., Vol. 30, p. 139.
[20] GUTKOWSKI, K I.; SHARIATI, A.; PETERS, C. J., High-pressure phase behavior of the binary ionic liquid system 1-octyl-3-methylimidazolium tetrafluoroborate + carbon dioxide, J. Supercrit. Fluid., Vol. 39. P. 187.
[21] TAGIURI, A. et al., Effect of cation on the solubility of carbon dioxide in three bis(fluorosulfonyl)imide low viscosity ([FSI]) ionic liquids, Fluid Phase Equilibr., Vol. 375, p. 324.
[22] MATTEDI, S. et al., High pressure CO_2 solubility in N-methyl-2-hydroxyethylammonium protic ionic liquids, J. Supercrit. Fluid., Vol. 56, p. 224.
[23] KURNIA, K. A. et al., Thermodynamic properties of CO_2 absorption in hydroxyl ammonium ionic liquids at pressures of (100–1600) kPa, J. Chem. Thermodyn., Vol. 41, p. 1069.
[24] YUAN, X. et al., Solubilities of CO_2 in hydroxyl ammonium ionic liquids at elevated pressures, Fluid Phase Equilibr., Vol. 257, p. 195.

[25] DIPPR Information and Data Evaluation Manager. Version 1.2.0, 2000.